Biochemical Pharmacology 78 (2009) 344–354

Contents lists available at ScienceDirect

Biochemical Pharmacology

journal homepage: www.elsevier.com/locate/biochempharm

Antimelanoma activity of the redox dye DCPIP (2,6-dichlorophenolindophenol) is antagonized by NQO1

Christopher M. Cabello, Warner B. Bair 3rd, Alexandra S. Bause, Georg T. Wondrak *

Department of Pharmacology and Toxicology, College of Pharmacy, Arizona Cancer Center, University of Arizona, 1515 North Campbell Avenue, Tucson, AZ 85724, USA

ARTICLE INFO

Article history:
Received 12 March 2009
Accepted 15 April 2009

Keywords:
Melanoma
Oxidative stress
NQO1
2,6-Dichlorophenolindophenol
Hsp70B'
Xenograft

ABSTRACT

Altered redox homeostasis involved in the control of cancer cell survival and proliferative signaling represents a chemical vulnerability that can be targeted by prooxidant redox intervention. Here, we demonstrate that the redox dye 2,6-dichlorophenolindophenol (DCPIP) may serve as a prooxidant chemotherapeutic targeting human melanoma cells *in vitro* and *in vivo*. DCPIP-apoptogenicity observed in the human melanoma cell lines A375 and G361 was inversely correlated with NAD(P)H:quinone oxidoreductase (NQO1) expression levels. In A375 cells displaying low NQO1 activity, DCPIP induced apoptosis with procaspase-3 and PARP cleavage, whereas G361 cells expressing high levels of enzymatically active NQO1 were resistant to DCPIP-cytotoxicity. Genetic (siRNA) or pharmacological (dicoumarol) antagonism of NQO1 strongly sensitized G361 cells to DCPIP apoptogenic activity. DCPIP-cytotoxicity was associated with the induction of oxidative stress and rapid depletion of glutathione in A375 and NQO1-modulated G361 cells. Expression array analysis revealed a DCPIP-induced stress response in A375 cells with massive upregulation of genes encoding *Hsp70B'* (HSPA6), *Hsp70* (HSPA1A), heme oxygenase-1 (HMOX1), and early growth response protein 1 (EGR1) further confirmed by immunodetection. Systemic administration of DCPIP displayed significant antimelanoma activity in the A375 murine xenograft model. These findings suggest feasibility of targeting tumors that display low NQO1 enzymatic activity using DCPIP.

1. Introduction

Recent research indicates that redox dysregulation in melanoma and other cancer cells represents a chemical vulnerability that can be targeted by small molecule redox chemotherapeutics with prooxidant activity. According to this hypothesis, prooxidant pharmacological agents substantially increase cellular reactive oxygen species (ROS) and thereby induce deviations from redox homeostasis that do not reduce viability of untransformed cells, but cannot be tolerated by malignant cells already under high constitutive oxidative stress [1–5]. A variety of small molecule prooxidants containing redox active pharmacophores, such as organic endoperoxides [6,7], Michael acceptor- and quinone-based electrophiles [8–11], and redox cyclers [12–14], have shown chemotherapeutic efficacy in cell culture-based systems and animal xenograft models [3,4]. In addition, anticancer activity of investigational prooxidant chemotherapeutics, including artemisinin [7,15], disulfiram [16], and elesclomol [17], is currently evaluated in advanced clinical trials [3,5,18].

Differential redox regulation between untransformed primary melanocytes and melanoma cells is known to alter proliferative and survival signaling through ROS-inhibition of the tumor suppressor phosphatase PTEN and ROS-activation of NFκB transcriptional activity, contributing to the notorious chemoresistance of metastatic melanoma and potentially providing a therapeutic opportunity for pharmacological redox intervention [5,19–21]. Led by the emerging chemotherapeutic benefit provided by experimental prooxidants, we aimed at the identification of promising redox pharmacophores with acceptable systemic toxicity profile that would target melanoma cells by induction of oxidative stress and focused our interest on the established redox dye 2,6-dichlorophenolindophenol {2,6-dichloro-4-[(p-hydroxyphenyl)imino]-2,5-cyclohexadien-1-one sodium salt, DCPIP; CAS #620-45-1}. This membrane-permeable dihalogenated 1,4-benzoquinoneimine-type oxidant (E'o (DCPIP) = +0.22 V; log *p* (octanol/water) = 0.13) is widely used as a specific standard substrate for the colorimetric determination of cellular NAD(P)H:quinone

Abbreviations: AV, annexinV; DC, dicoumarol; DCPIP, 2,6-dichlorophenolindophenol; DDIT3, DNA-damage-inducible transcript 3; EGR1, early growth response gene 1; FITC, fluorescein isothiocyanate; GADD45A, growth arrest and DNA-damage-inducible alpha; GSH, glutathione; Hsp, heat shock protein; HMOX1, heme oxygenase-1; NAC, N^{α}-acetyl-L-cysteine; NQO1, NAD(P)H:quinone oxidoreductase 1; PARP, poly(ADP-ribose) polymerase; PI, propidium iodide; q.d., quaque die/every day; ROS, reactive oxygen species; SDS-PAGE, sodium dodecylsulfate polyacrylamide gel electrophoresis.

* Corresponding author. Tel.: +1 520 626 9017; fax: +1 520 626 8567.
E-mail address: wondrak@pharmacy.arizona.edu (G.T. Wondrak).

0006-2952/$ – see front matter © 2009 Elsevier Inc. All rights reserved.
doi:10.1016/j.bcp.2009.04.016

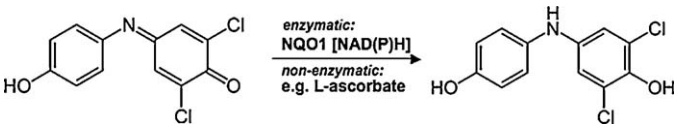

Fig. 1. The dihalogenated benzoquinoneimine redox dye 2,6-dichlorophenolindophenol (DCPIP). Reduction of the blue dye DCPIP (λ_{max} = 600 nm) with formation of the colorless p-aminophenol hydroquinone leuco form occurs through enzymatic transformation by NAD(P)H quinone oxidoreductase (NQO1) or nonenzymatic reaction with reducing agents such as ascorbic acid.

oxidoreductase (NQO1; EC 1.6.99.2, also referred to as DT-diaphorase) enzymatic activity, thereby reductively converted into the hydroquinone-leucoform [23,24]; DCPIP also serves as an oxidizing reactant (Tillman's reagent) for analytical redox titration of the reducing agent L-ascorbic acid (Fig. 1) [25]. As a redox probe DCPIP can serve as an electron acceptor for electron carriers of the mitochondrial respiratory chain and as a substrate (Hill reagent) for chloroplast-mediated photoreduction [26–28]. Importantly, other simple quinone systems with related redox chemistry including menadione [E'o (menadione) = +0.14 V] have shown efficacy as prooxidant experimental cancer chemotherapeutics [8], and antimelanoma activity of N-acetyl-para-aminophenol (acetaminophen) tested in ongoing clinical studies has recently been attributed to glutathione depletion by the tyrosinase-derived o-quinone-metabolite [29,30].

Based on prooxidant redox reactivity and drug-like properties of DCPIP that include chemical stability, systemic deliverability, membrane permeability, and low systemic toxicity established earlier in mice (LD_{50} = 180 mg/kg; intravenous administration [31]), we tested feasibility of using this 1,4-benzoquinoneimine-derivative as an experimental redox chemotherapeutic targeting human melanoma cells *in vitro* and *in vivo*. Here we demonstrate that (I) DCPIP induces apoptosis in cultured melanoma cells associated with upregulation of cellular oxidative stress and oxidative stress-induced gene expression, that (II) DCPIP cytotoxicity in human melanoma cell lines is inversely correlated with NQO1 expression levels, and that (III) systemic administration of DCPIP displays significant antimelanoma activity in an animal model of the disease.

2. Materials and methods

2.1. Materials

All chemicals were purchased from Sigma Chemical Co (St. Louis, MO, USA). The cell-permeable pancaspase inhibitor Z-VAD-(OMe)-fmk was from Calbiochem-Novabiochem (San Diego, CA, USA).

2.2. General cell culture

G-361 Human metastatic melanoma cells from ATCC (Manassas, VA, USA) were cultured in McCoy's 5a medium containing 10% bovine calf serum (BCS). A375 human metastatic melanoma cells (ATCC) were cultured in RPMI medium containing 10% BCS and 2 mM L-glutamine. Cells were maintained at 37 °C in 5% CO_2, 95% air in a humidified incubator.

2.3. Human melanoma SCID mouse xenograft model

A375 human melanoma cells were grown in HyQ RPMI-1640 media supplemented with 10% fetal bovine serum, and maintained in 5% CO_2–95% air humidified atmosphere at 37 °C. Subconfluent cells were harvested by using 0.25% trypsin-EDTA. Cells (>90% viability) were resuspended at the concentration of 10×10^6 cells/100 μl of sterile saline. A SCID mouse colony was developed at the University of Arizona using original SCID (C.B-17/IcrACCSCID) obtained from Taconic (Germantown, NY, USA). The mice were housed in microisolator cages (Allentown Caging Equipment Company, Allentown, NJ, USA) and maintained under specific pathogen-free conditions. Every month mice were screened by ELISA serology for mycoplasma, mouse hepatitis virus, pinworms, and Sendai virus and tested negative. SCID mice 6–8 weeks of age were bled (<200 μl) by retroorbital puncture in order to screen for the presence of mouse IgG using an ELISA. Only mice with IgG levels ≤20 μg/ml were used for the experiments. The mice ate NIH-31 irradiated pellets (Tekland Premier, Madison, WI, USA) and received autoclaved water. Animal facilities are approved by the Association for the Assessment and Accreditation of Laboratory Animal Care International and in accordance with United States Department of Agriculture, Department of Health and Human Services, and NIH regulations. A375 cell injections (10×10^6 cells) were given subcutaneously on the mouse's lower right flank on day 0, and after tumors became established (~65 mm^3) mice were pair-matched into the treatment groups. The following day, treatment with PBS or PBS only was initiated. The chemotherapeutic test agent DCPIP (1 mg/ml PBS) was prepared and administered by intraperitoneal injection in less than 1 h. DCPIP (low dose group: 4 mg/kg/d, 100 μl, q.d., n = 12; high dose group: 16 mg/kg/d, 200 μl, b.i.d., n = 11) was given on days 1–7 and 10–12 post the day of pair-matching, whereas control animals received carrier only (PBS, 200 μl, b.i.d., n = 12). Subcutaneous tumors were measured twice weekly for tumor volume estimation (mm^3) in accordance with the formula $(a^2 \times b)/2$ where a is the smallest diameter and b is the largest diameter. The mice were sacrificed individually by CO_2 when the tumors reached a volume of 2000 mm^3. Tumor growth curves were obtained by determining average tumor volumes until day 30 after cell injection, and data points were analyzed using the two-sided Student's t-test ($^*p < 0.05$; $^{**}p < 0.01$; $^{***}p < 0.001$). All procedures were completed in accordance with the University of Arizona Institutional Animal Care and Use Committee (IACUC) protocol (#07-029, approved 24 May 2007).

2.4. Cell proliferation assay

Cells were seeded at 10,000 cells/dish on 35-mm dishes. After 24 h, cells were treated with test compound. Cell number at the time of compound addition and 72 h later were determined using a Z2 Analyzer (Beckman Coulter, Inc., Fullerton, CA, USA). Proliferation was compared with cells that received mock treatment. The same methodology was used to establish IC_{50} values (drug concentration that induces 50% inhibition of proliferation of treated cells within 72 h exposure ± SD, n = 3) of anti-proliferative potency.

2.5. Apoptosis analysis

Viability and induction of cell death (early and late apoptosis/necrosis) were examined by annexin-V-FITC/propidium iodide (PI) dual staining of cells followed by flow cytometric analysis as published previously [32]. Cells (100,000) were seeded on 35 mm dishes and received drug treatment 24 h later. Cells were harvested at various time points after treatment and cell staining was performed using an apoptosis detection kit according to the manufacturer's specifications (APO-AF, Sigma, St. Louis, MO, USA).

2.6. Caspase-3 activation assay

Treatment-induced caspase-3 activation was examined in A375 melanoma cells using a cleaved/activated caspase-3 (asp 175)

antibody (Alexa Fluor 488 conjugate, Cell Signaling, Danvers, MA, USA) followed by flow cytometric analysis as published recently [14]. Briefly, cells were harvested 24 h after treatment, resuspended in PBS and fixed in 1% formaldehyde. Cells were then permabilized using 90% methanol and resuspended in incubation buffer (PBS, 0.5% BSA). After rinsing by centrifugation, cells were resuspended in incubation buffer (90 μl) and cleaved caspase-3 antibody (10 μl) was added. After incubation (40 min) followed by rinsing and centrifugation in incubation buffer, cells were resuspended in PBS and analyzed by flow cytometry.

2.7. PARP immunoblot analysis

Cells were treated with 40 μM DCPIP for 24 h and lysed with RIPA buffer (100 μl, 50 mM Tris–HCl, pH 7.4, 150 mM NaCl, 1 mM EDTA, 25% deoxycholic acid, and 1% NP-40). After sample separation (30 μg protein) by SDS-PAGE (4–15% gradient gel, Bio-Rad, Hercules, CA, USA), semidry transfer onto a nitrocellulose membrane (Optitran, Whatman, Bedford, MA, USA) was performed, followed by incubation in blocking buffer [PBST (0.1% Tween 20), 5% nonfat dry milk] for 1 h at 25 °C. Membranes were washed three times with PBST and incubated overnight at 4 °C with a monoclonal rabbit anti-PARP antibody diluted 1:1000 (46D11, Cell Signaling, Danvers, MA, USA) in incubation buffer (PBST, 5% BSA). Membranes were washed three times with PBST followed by incubation for 1 h at 25 °C with HRP-linked anti-rabbit IgG antibody (Cell Signaling) diluted 1:2000 in blocking buffer. Visualization occurred by enhanced chemiluminescence.

2.8. Heme oxygenase-1 (HO-1) immunoblot analysis

One day before treatment, 2×10^6 cells were seeded in T-75 flasks. Cell growth medium was replaced 24 h after seeding, followed by addition of test compounds 60 min after medium change. Cells were incubated for 24 h (37 °C, 5% CO_2), then washed with PBS, lysed in 1× SDS-PAGE sample buffer (200 μl, 0.375 M Tris–HCl pH 6.8, 50% glycerol, 10% SDS, 5% β-mercaptoethanol, 0.25% bromophenol blue), and heated for 3 min at 95 °C. Samples (10 μl, containing approximately 45 μg total protein as determined by the BCA assay) were separated by 15% SDS-PAGE followed by immediate transfer to nitrocellulose membranes (Optitran, Whatman, Piscataway, NJ, USA). The membrane was blocked with 5% milk in 0.1% PBST for 1 h. Rabbit anti-HO-1 polyclonal antibody (Stressgen Bioreagents, Ann Arbor, MI) was used 1:5000 in 5% milk-PBST overnight at 4 °C. The membrane was washed three times for 10 min in 0.1% PBST before adding HRP-conjugated goat anti-rabbit antibody (Jackson Immunological Research, West Grove, PA, USA) at 1:10,000 dilution followed by visualization using enhanced chemiluminescence detection reagents. Equal protein loading was examined by α-actin-detection using a mouse anti-actin monoclonal antibody (Sigma) at 1:1500 dilution.

2.9. NQO1 immunoblot analysis

Cell extraction, separation by 12% SDS-PAGE, and Western analysis were performed as specified for HO-1. Immunoblot analysis was performed using a mouse anti-NQO1 monoclonal primary antibody (Abcam, Cambridge, MA, USA; 1:1000 dilution) and an HRP-conjugated goat anti-mouse secondary antibody (Jackson Immunological Research; 1:10,000 dilution).

2.10. Early growth response-1 (EGR-1) immunoblot analysis

Cell extraction, separation by 12% SDS–PAGE, and Western analysis were performed as specified for HO-1. Rabbit anti-EGR1 monoclonal primary antibody (44D5, Cell Signaling; 1:2000 dilution) and HRP-conjugated anti-rabbit IgG secondary antibody (Cell Signaling; 1:1500 dilution) were used.

2.11. Hsp70B' ELISA

The enzyme-linked immunosorbent assay for Hsp70B' was performed in 96 well format on cell lysates extracted from treated cells following kit instructions (Assay Designs, Inc., Ann Arbor, MI, USA). Briefly, 1×10^6 cells were seeded per T-75 flask 1 day before treatment. Cell growth medium was replaced 24 h after seeding, followed by addition of test compound 60 min after medium change. Cells (3×10^6 per group) were incubated for 24 h (37 °C, 5% CO_2) and then harvested, washed with PBS, and lysed in 1× extraction reagent. After protein quantification using the BCA assay, samples were diluted to a range within the Hsp70B' standard curve and processed according to the manufacturer's instructions. Absorbance (450 nm) was determined on a microtiter plate reader (Versamax, Molecular Devices, Sunnyvale, CA, USA). Data represent the average of three independent experiments.

2.12. Measurement of NQO1-specific activity

Determination of NQO1 specific activity was performed according to a published standard procedure [14]. In brief, cells (2×10^6) were harvested by trysinization and resuspended in ice-cold TE (20 mM Tris–HCl with 2 mM EDTA, pH 7.4). Cells were disrupted in three cycles of freeze/thawing using liquid nitrogen and a 37 °C waterbath, followed by centrifugation (12,000 × *g*, 5 min). Protein concentration in the supernatant was determined using the BCA assay (Pierce, Rockford, IL, USA). For determination of NQO1 specific activity the reaction mixture (1 ml final volume) contained: 25 mM Tris–HCl (pH 7.4), 180 μM NADPH, BSA (0.2 mg/ml), Tween 20 [0.01% (v/v)], and cell lysate (5 μl). The reaction was started by the addition of 2 μl 2,6-dichlorophenolindophenol (DCPIP, 20 mM stock in DMSO). Reduction of DCPIP was measured at room temperature for 1 min at 600 nm ($\varepsilon = 21 \times 10^3\ M^{-1}\ cm^{-1}$) with or without 20 μM dicoumarol. The dicoumarol-inhibitable part of DCPIP reduction was used to calculate NQO1 activity expressed as nmol DCPIP/mg protein/min. A minimum of triplicate cultures were assayed.

2.13. Detection of intracellular oxidative stress by flow cytometric analysis

Induction of intracellular oxidative stress by DCPIP was analyzed by flow cytometry using 2′,7′-dichlorodihydrofluorescein diacetate (DCFH-DA) as a sensitive non-fluorescent precursor dye according to a published standard procedure [14]. Human A375 melanoma cells were treated with DCPIP (10, 20, and 40 μM, 24 h) followed by DCFH-DA loading. To this end, cells were incubated for 60 min in the dark (37 °C, 5% CO_2) with culture medium containing DCFH-DA (5 μg/ml final concentration). Cells were then harvested, washed with PBS, resuspended in 300 μl PBS and immediately analyzed by flow cytometry.

2.14. Determination of total cellular glutathione content

Pharmacological modulation of intracellular glutathione content was analyzed using the photometric HT Glutathione Assay Kit (Trevigen, Gaithersburg, MD, USA) performed in 96 well format. This kinetic assay is based on the enzymatic recycling method involving glutathione reductase and DTNB (5,5′-dithiobis-2-nitrobenzoic acid, Ellman's reagent) to produce yellow colored 5-thio-2-nitrobenzoic acid (TNB) that absorbs at 405 nm. Human A375 melanoma (1×10^6) cells were exposed to DCPIP (40 μM,

6 h) and harvested by trypsinization followed by sample processing according to the manufacturer's instructions. Oxidized glutathione was determined separately after 4-vinylpyridine-derivatization. Glutathione content of total cellular extracts was normalized to protein content determined using the BCA assay (Pierce, Rockford, IL, USA).

2.15. siRNA transfection and NQO1 expression analysis by real time RT-PCR

G361 cells were transiently transfected with a 100 nM pool of four siRNA oligonucleotides targeting NQO1 or a 100 nM pool of four non-targeting siRNA oligonucleotides using the DharmaFECT 1 transfection reagent (Dharmacon RNA Technologies, Lafayette, CO, USA). The sequences of siGENOME NQO1 SMARTpool (NQO1 siRNA) [GenBank: NM 001025434] were GAAAGGACAUCACAG-GUAA; GAAGGACCCUGCGAACUUU; GCAAGUCCAUCCCAACUGA; and CCGACUCUGUUCUGGCUUA. The oligos were resuspended in the Dharmacon 1× siRNA buffer and incubated in serum free media for 5 min. DharmaFECT 1 was also incubated in serum free media for 5 min prior to the addition of the siRNA oligos. The oligos were incubated with the transfection reagent for 20 min prior to cellular treatment. Complete media was added to the siRNA oligo mixture and the cells were incubated with the siRNAs in appropriate cell culture conditions for 72 h. Cells were than re-transfected with another 100 nM pool of four siRNA oligonucleotides targeting NQO1 or a 100 nM pool of four non-targeting siRNA oligonucleotides. Twenty-four hours after the second transfection, cells were either harvested for expression analysis or plated for subsequent DCPIP treatment. For NQO1 expression analysis by real time RT-PCR, total cellular RNA (3×10^6 cells) was prepared using the RNEasy kit from Qiagen (Valencia, CA, USA). Reverse transcription was performed using TaqMan Reverse Transcription Reagents (Roche Molecular Systems, Branchburg, NJ, USA) and 200 ng of total RNA in a 50-μl reaction. Reverse transcription was primed with random hexamers and incubated at 25 °C for 10 min followed by 48 °C for 30 min, 95 °C for 5 min, and a chill at 4 °C. Each PCR reaction consisted of 3.75 μl of cDNA added to 12.5 μl of TaqMan Universal PCR Master Mix (Roche Molecular Systems), 1.25 μl of gene-specific primer/probe mix (Assays-by-Design; Applied Biosystems, Foster City, CA) and 7.5 μl of PCR water. PCR conditions were: 95 °C for 10 min, followed by 40 cycles of 95 °C for 15 s, alternating with 60 °C for 1 min using an Applied Biosystems 7000 SDS and Applied Biosystems' Assays On Demand primers specific to NQO1 (assay ID Hs00168547_m1) and GAPDH (assay ID Hs99999905_m1). Gene-specific product was normalized to GAPDH and quantified using the comparative ($\Delta\Delta C_t$) Ct method as described in the ABI Prism 7000 sequence detection system user guide [11]. Expression values were averaged across three independent experiments, and standard deviation was calculated for graphing.

2.16. Human stress and toxicity pathfinder™ RT² profiler™ PCR expression array

After pharmacological exposure, total cellular RNA (3×10^6 A375 melanoma cells) was prepared according to a standard procedure using the RNeasy kit (Qiagen, Valencia, CA, USA). Reverse transcription was performed using the RT² First Strand kit (Superarray, Frederick, MD, USA) and 5 μg total RNA. The RT² Human Stress and Toxicity Pathfinder™ PCR Expression Array (SuperArray) profiling the expression of 84 stress-related genes was run using the following PCR conditions: 95 °C for 10 min, followed by 40 cycles of 95 °C for 15 s alternating with 60 °C for 1 min (Applied Biosystems 7000 SDS). Gene-specific product was normalized to GAPDH and quantified using the comparative ($\Delta\Delta C_t$) Ct method as described in the ABI Prism 7000 sequence detection system user guide. Expression values were averaged across three independent array experiments, and standard deviation was calculated for graphing.

2.17. Statistical analysis

Unless indicated differently, the results are presented as mean ± SD of at least three independent experiments. They were analyzed using the two-sided Student's *t*-test ($^*p < 0.05$; $^{**}p < 0.01$; $^{***}p < 0.001$).

3. Results

3.1. DCPIP induces apoptosis with procaspase-3 and PARP cleavage in cultured human A375 melanoma cells

First, the dose-response of induction of A375 melanoma cell death by exposure to DCPIP was assessed by flow cytometric analysis of annexinV-FITC/propidium iodide-stained cells (Fig. 2A). Exposure to DCPIP at concentrations higher than 10 μM for 24 h induced pronounced apoptosis that could be suppressed significantly by pretreatment (1 h) with the pancaspase inhibitor zVAD-fmk added before DCPIP exposure suggesting a caspase-dependent mode of DCPIP-induced cell death. This finding was confirmed, when cleavage of procaspase-3 and PARP, important markers of induction of apoptosis, were examined in A375 cells exposed to increasing doses of DCPIP (10, 20, and 40 μM, 24 h exposure) (Fig. 2B and C, respectively). At 20 and 40 μM DCPIP (24 h exposure) pronounced cleavage of procaspase 3 was detected (Fig. 2B), and complete PARP cleavage was observed (40 μM, 24 h) (Fig. 2C). Taken together, these findings demonstrate that DCPIP treatment at lower micromolar concentrations induces apoptotic cell death in A375 melanoma cells.

3.2. Exposure to the combined action of DCPIP and the NQO1 inhibitor dicoumarol induces apoptosis in cultured human G361 melanoma cells

In contrast to A375 melanoma cells, human G361 metastatic melanoma cells displayed a marked resistance to induction of apoptosis by DCPIP as assessed by flow cytometric analysis of annexinV-FITC/propidium iodide-stained cells after 24 h exposure to up to 40 μM DCPIP (Fig. 3A, upper panels). Similar results that support preferential DCPIP-sensitivity of A375 versus G361 melanoma cells were obtained when inhibition of cell proliferation in response to DCPIP treatment [IC_{50} (μM): 1.9 ± 0.5 (A375); 19.3 ± 3.1 (G361), 72 h continuous exposure] was assessed (data not shown). Based on the established reductive metabolism of DCPIP by NQO1 [23], a flavoprotein that catalyzes the two-electron reduction of various quinones and quinone imines using NAD(P)H, thereby preventing semiquinone-dependent redox cycling and facilitating conjugation and systemic excretion [22,33], we tested the hypothesis that NQO1-inhibition would sensitize G361 melanoma cells to DCPIP treatment. Indeed, pronounced induction of apoptosis was achieved in G361 cells exposed to the combined action of the NQO1-inhibitor dicoumarol (DC) and DCPIP (Fig. 3A, lower panels). Importantly, exposure to dicoumarol only (up to 60 μM, 24 h) was not associated with any cytotoxicity. Consistent with our earlier findings demonstrating high specific enzymatic activity of NQO1 in G361 cells (2403 ± 215 nmol DCPIP/mg protein/min, $n = 3$) and low specific enzymatic activity in A375 cells (283 ± 37 nmol DCPIP/mg protein/min, $n = 3$) [14], Western blot analysis confirmed differential expression levels of NQO1 in these two metastatic melanoma cell lines (Fig. 3B). Taken together, these findings suggest that DCPIP cytotoxicity may be modulated by cellular expression and enzymatic

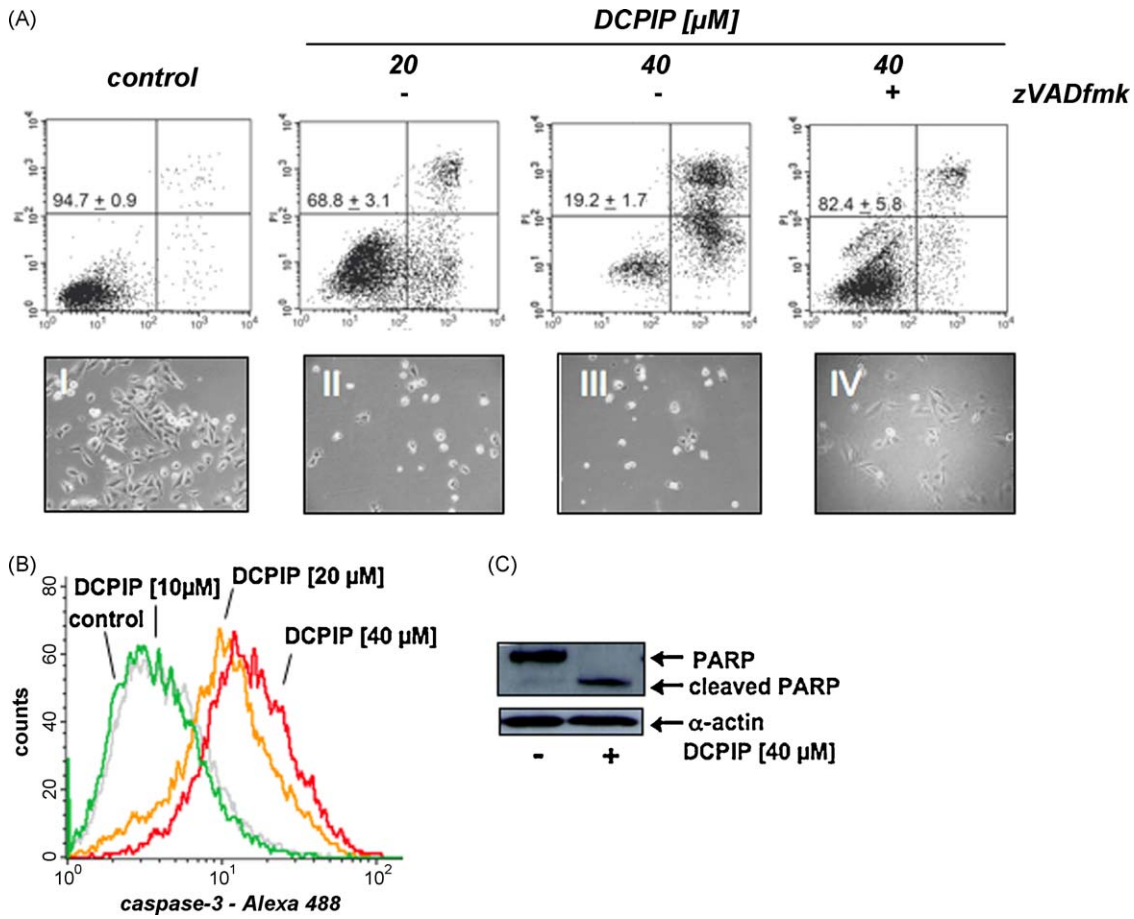

Fig. 2. Exposure to DCPIP dose-dependently induces apoptosis with cleavage of procaspase-3 and PARP in human A375 melanoma cells. (A) Induction of cell death by exposure to increasing doses of DCPIP (20 and 40 μM, 24 h) in the absence or presence of the pancaspase inhibitor zVADfmk was assessed by flow cytometric analysis of annexinV-FITC/propidium iodide-stained cells. The numbers indicate viable cells (AV^-, PI^-, lower left quadrant) in percent of total gated cells (mean ± SD, $n = 3$). Representative light microscopy pictures taken after 24 h exposure to DCPIP are shown in panels I–IV. (B) DCPIP-induced (10, 20, and 40 μM, 24 h) caspase-3 activation was examined by flow cytometric detection using an Alexa Fluor 488-conjugated monoclonal antibody against cleaved procaspase-3. One representative experiment of three similar repeats is shown. (C) DCPIP-induced (40 μM, 24 h) PARP cleavage was examined by immunoblot analysis.

activity of the quinone-detoxifying enzyme NQO1, i.e. differential sensitivity to DCPIP apoptogenicity as observed in A375 and G361 melanoma cells may result from differential expression levels of NQO1 and may be modulated by pharmacological NQO1 inhibition.

3.3. Genetic antagonism of NQO1 sensitizes G361 human melanoma cells to DCPIP apoptogenic activity

Based on our experiments using the pharmacological inhibitor dicoumarol as a molecular probe for the involvement of NQO1 enzymatic activity in the reductive detoxification of the quinoneimine DCPIP, we further examined the role of NQO1 in DCPIP chemoresistance using a specific genetic approach based on siRNA-mediated target modulation (Fig. 4). Knockdown of NQO1 gene expression was confirmed by real time RT-PCR analysis indicating downregulation of NQO1 mRNA by approximately 5-fold when compared to control siRNA transfected A375 cells (Fig. 4B). Western-analysis further confirmed the substantial downregulation of NQO1 protein levels (Fig. 4C) that was also apparent from an approximately 4-fold reduction of NQO1 specific enzymatic activity detected in cell protein extracts prepared from siNQO1-treated (24.5 ± 0.6% of wildtype activity, $n = 3$, $p < 0.001$) versus siControl-treated (110.7 ± 3.7% of wildtype, $n = 3$, $p < 0.05$) and untreated wildtype cells (100.0 ± 3.5%, $n = 3$). Remarkably, NQO1 knockdown (Fig. 4A, lower panels), but not treatment with siControl (Fig. 4A, middle panels), resulted in pronounced DCPIP-chemosensitization of G361 melanoma cells (Fig. 4A, upper panels) confirming the results obtained with the pharmacological NQO1-inhibitor dicoumarol (Fig. 3A).

In summary, our data obtained from pharmacological and genetic target modulation studies strongly suggest that DCPIP apoptogenic potency observed in human A375 and G361 melanoma cells is a function of cellular NQO1 expression levels.

3.4. DCPIP induces oxidative stress with rapid depletion of cellular glutathione in A375 and NQO1-modulated G361 melanoma cells

Based on earlier work that has demonstrated the involvement of oxidative stress in mediating the cytotoxic effects of redox quinones [8,22,30,34,35], we examined the role of cellular oxidative stress and redox alterations in DCPIP apoptogenicity (Fig. 5). First, a dose-dependent elevation of intracellular oxidative stress could be observed in A375 melanoma cells exposed to DCPIP (10, 20, and 40 μM, 24 h) as assessed by 2′,7′-dichloro-dihydro-fluorescein diacetate detection of intracellular peroxides using flow cytometry (Fig. 5A). Consistent with a mechanistic involvement of oxidative stress in the induction of apoptosis by DCPIP, preincubation (24 h) of A375 cells with the antioxidant and glutathione precursor N^{α}-acetyl-L-cysteine (NAC, 10 mM) strongly suppressed DCPIP-induced procaspase 3 cleavage (Fig. 5B). In addition, modulation of cellular glutathione levels in A375 and G361 melanoma cells exposed to DCPIP (40 μM) was examined at

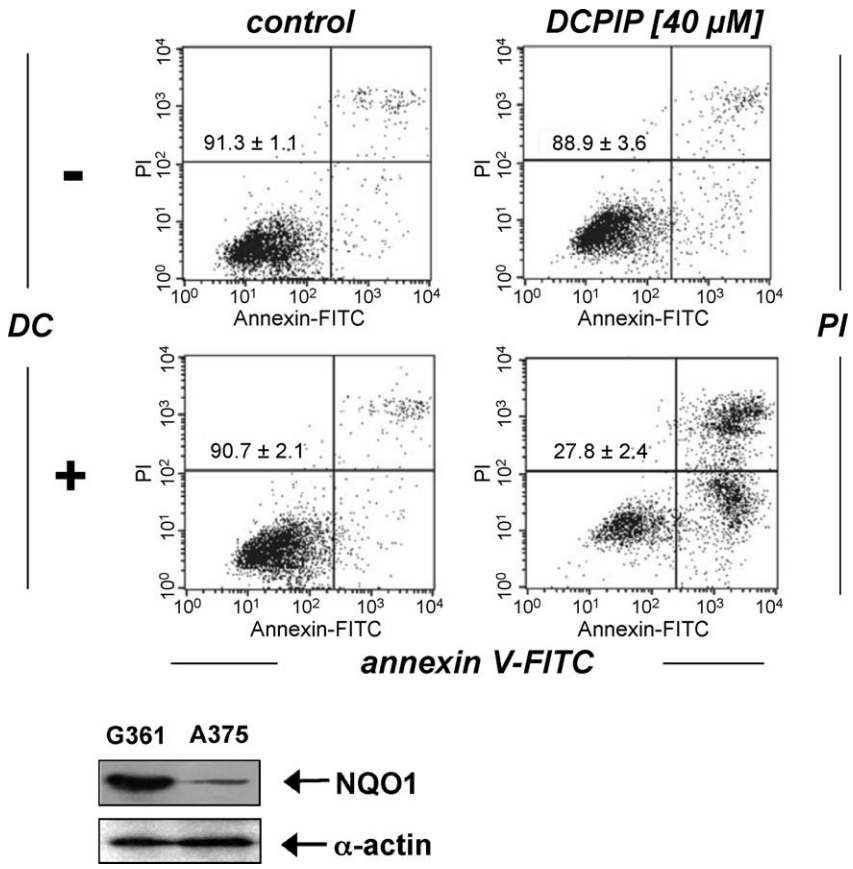

Fig. 3. Dicoumarol treatment sensitizes human G361 melanoma cells to DCPIP-induced apoptosis. (A) Induction of cell death by exposure to DCPIP (40 μM, 24 h) in the absence or presence of the NQO1 inhibitor dicoumarol (DC, 60 μM) was assessed by flow cytometric analysis of annexinV-FITC/propidium iodide-stained cells. The numbers indicate viable cells (AV^-, PI^-, lower left quadrant) in percent of total gated cells (mean ± SD, $n = 3$). (B) NQO1 protein levels in G361 and A375 cells were compared by immunoblot analysis.

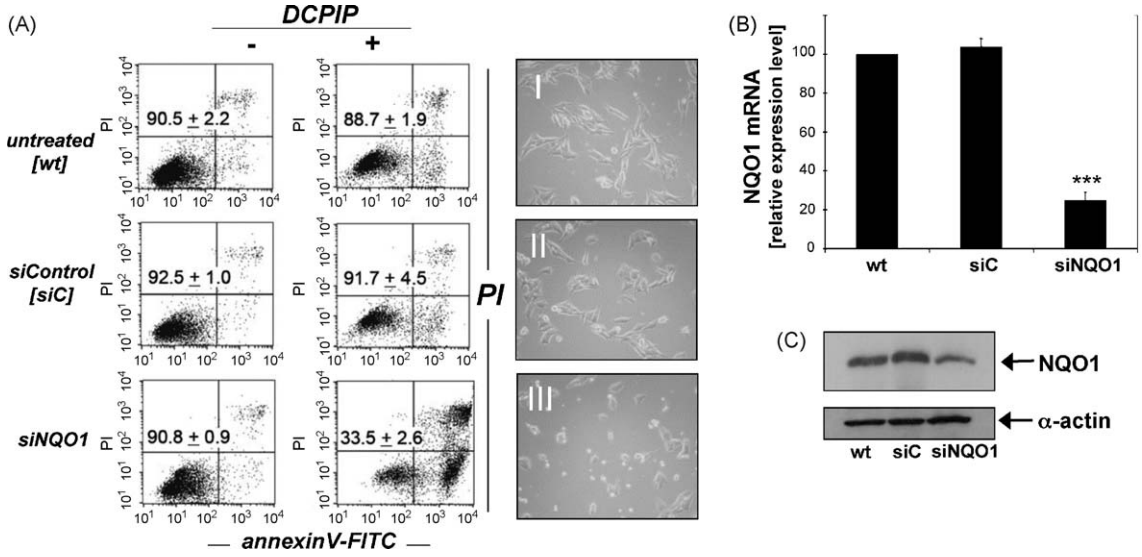

Fig. 4. Genetic downregulation of NQO1 expression sensitizes human G361 melanoma cells to DCPIP-induced apoptosis. (A) Induction of cell death by exposure to DCPIP (40 μM, 24 h) was examined in G361 wild type cells (untreated, wt) and after control siRNA treatment (siControl, siC) and NQO1 siRNA knockdown (siNQO1). The numbers indicate viable cells (AV^-, PI^-, lower left quadrant) in percent of total gated cells (mean ± SD, $n = 3$). Representative light microscopy pictures taken after 24 h exposure to DCPIP are shown in panels I–III. (B) NQO1-Knockdown was confirmed by expression analysis using quantitative RT-PCR (mean ± SD, $n = 3$) and (C) immunoblot analysis as specified in Section 2.

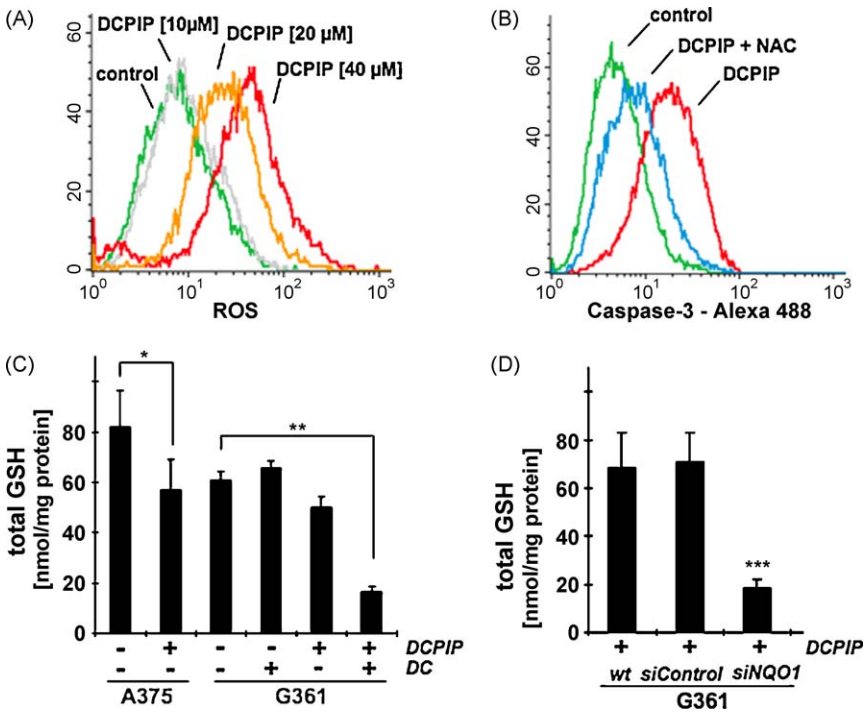

Fig. 5. DCPIP induces oxidative stress in human melanoma cell lines. (A) Induction of intracellular oxidative stress in human A375 melanoma cells by treatment with DCPIP. Cells were exposed to DCPIP (10, 20, 40 μM, 24 h) and intracellular oxidative stress was assessed by 2′,7′-dichloro-dihydrofluorescein diacetate staining followed by flow cytometric analysis. One representative experiment of three similar repeats is shown. (B) Antioxidant protection against DCPIP-induced caspase-3 activation. Cells were pretreated with NAC (10 mM, 24 h) or left untreated. After medium change, DCPIP (40 μM) was added and caspase-3 activation was examined after another 24 h by flow cytometric detection using an Alexa Fluor 488-conjugated monoclonal antibody against cleaved procaspase-3. One representative experiment of three similar repeats is shown. (C) Modulation of intracellular glutathione content in A375 and G361 melanoma cells exposed to DCPIP (40 μM, 6 h) in the absence or presence of DC (60 μM). Total glutathione content was normalized to protein content. (D) For NQO1 knockdown, G361 melanoma cells were treated with siNQO1- or siControl or left untreated as described in Section 2. Intracellular glutathione content was then determined in G361 melanoma cells exposed to DCPIP (40 μM, 6 h). Total glutathione content was normalized to protein content (mean ± SD, $n = 3$).

an early time point (6 h) in order to assess treatment-induced glutathione depletion that occurs independent of plasma membrane permeabilization observed at later time points during advanced stages of apoptosis (Fig. 5C and D). In A375 cells, DCPIP treatment reduced cellular glutathione levels by approximately 30%, whereas in G361 cells DCPIP-induced GSH depletion did not reach the level of statistical significance. In contrast, G361 glutathione levels were strongly reduced by approximately 70% when DCPIP treatment occurred in the presence of the NQO1 inhibitor dicoumarol (Fig. 5C). Importantly, no glutathione depletion occurred upon exposure to dicoumarol only. Genetic antagonism of NQO1 employing the siRNA methodology described above (Fig. 4) strongly sensitized G361 melanoma cells to the glutathione-depleting effects of DCPIP (Fig. 5D) consistent with a protective role of NQO1 against DCPIP cytotoxicity and glutathione depletion.

Taken together these data suggest that induction of oxidative stress, as evidenced by upregulation of cellular peroxide levels combined with glutathione depletion and antioxidant suppression of DCPIP-induced caspase 3 activation, is associated with DCPIP-induced cytotoxicity in human A375 cells. In G361 cells DCPIP-induced glutathione depletion was observed only after pharmacological or genetic antagonism of NQO1 enzymatic activity.

3.5. DCPIP induces a broad oxidative stress response in human A375 melanoma cells

After demonstrating apoptogenic and prooxidant activity of DCPIP in simple melanoma cell culture models, modulation of stress and toxicity response gene expression was examined in A375 human melanoma cells exposed to DCPIP. The RT^2 Human Stress and Toxicity Profiler^{TM} PCR Expression Array technology (SuperArray, Frederick, MD) was applied to A375 cells exposed to DCPIP (40 μM, 24 h exposure) to assess expression of 84 stress-related genes contained on the array (Fig. 6A, left panel). DCPIP-induced gene expression changes in A375 human melanoma cells affected 15 genes on the array by at least 3-fold over untreated control cells as summarized in Fig. 6A (right panel). Genes that were more than 10-fold upregulated encoded the oxidative stress responsive *heat shock proteins Hsp70B'* (HSPA6; 306-fold) and *Hsp70* (HSPA1A; 16-fold) [36], the heat shock protein and antioxidant enzyme *heme oxygenase-1* (HMOX1; 42-fold), the oxidative stress-responsive transcription factor and tumor suppressor *early growth response protein 1* (EGR1; 14-fold) [37], and *lymphotoxin-alpha* (LTA; 14-fold), an apoptogenic member of the tumor necrosis factor family [38]. Moreover, the stress- and DNA-damage response genes *DNA-damage-inducible transcript 3* (DDIT3) and *growth arrest and DNA-damage-inducible alpha* (GADD45A) were upregulated by approximately 4-fold in response to DCPIP exposure [39,40].

Next, DCPIP-induced upregulation of cellular HMOX1, EGR1, and HSPA6 gene expression was examined at the protein level by immunoblot or ELISA analysis, respectively (Fig. 6B–D). Consistent with a role in early redox stress response, pronounced upregulation of cellular EGR1 protein levels was detected within 3 h exposure to DCPIP, but returned to very low background levels over the next 9 h (Fig. 6B). Within 24 h, cellular heme oxygenase-1 protein levels were strongly upregulated upon exposure to DCPIP (20 and 40 μM, Fig. 6C). Protein levels of Hsp70B', the HSPA6 gene product, were also strongly upregulated as assessed by ELISA analysis (Fig. 6D). Significant induction was observed starting at 10 μM DCPIP, and higher than 100-fold upregulated protein

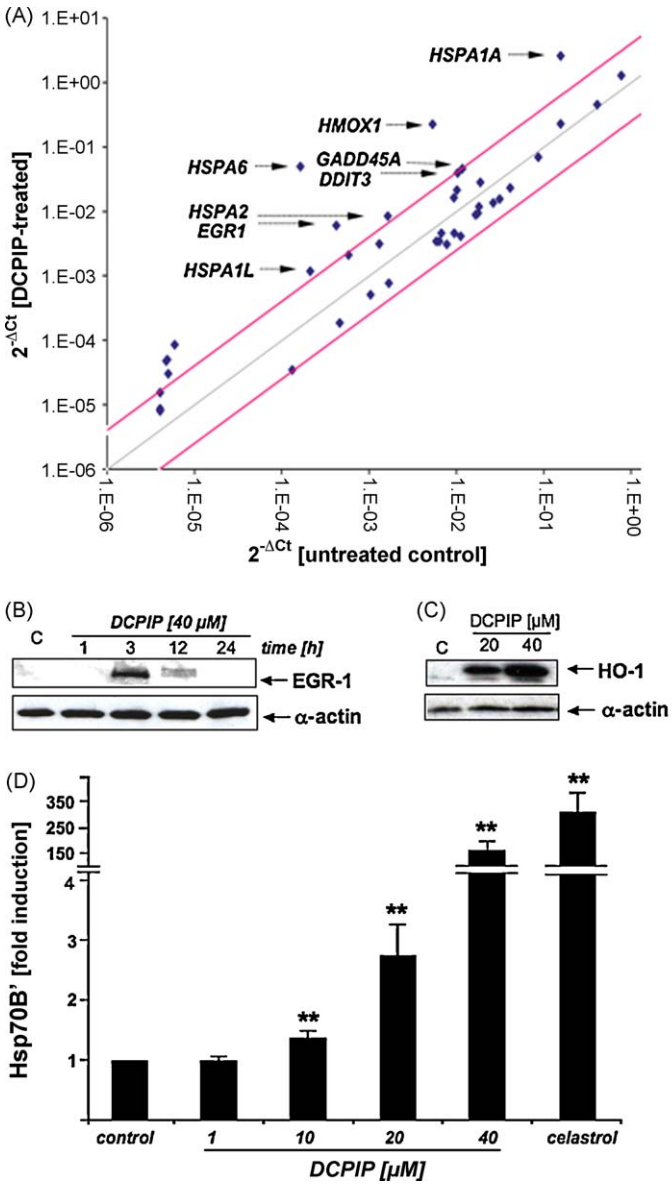

Gene Symbol	Fold Change	p-value
HSPA6 (NM_002155)	306.2	0.001
HMOX1 (NM_002133)	42.7	0.001
HSPA1A (NM_00345)	16.8	0.001
LTA (NM_000595)	14.6	0.001
EGR1 (NM_001964)	14.5	0.001
TNF (NM_000594)	10.3	0.001
CYP7A1 (NM_000780)	10.2	0.004
CCL3 (NM_002983)	6.1	0.043
HSPA1L (NM_005345)	5.7	0.001
HSPA2 (NM_021979)	5.2	0.001
GADD45A (NM_001924)	4.0	0.005
CCL4 (NM_002984)	3.9	0.012
DDIT3 (NM_004083)	3.9	0.013
GDF15 (NM_004864)	3.7	0.018
CCNG1 (NM_004060)	-3.7	0.006

Fig. 6. DCPIP induces oxidative stress and heat shock response gene expression in human A375 melanoma cells. (A) DCPIP-induced gene expression changes in A375 human melanoma cells. The scatter blot (left panel) depicts differential gene expression as detected by the RT^2 Human Stress and Toxicity Profiler^{TM} PCR Expression Array technology profiling the expression of 84 (oxidative) stress- and toxicity-related genes after DCPIP treatment (40 μM, 24 h). Upper and lower lines represent the cut-off indicating 3-fold up- or downregulated expression, respectively. Arrows specify selected genes with at least 4-fold upregulated expression versus untreated controls. Expression array analysis was performed in three independent repeats and analyzed using the two-sided Student's *t*-test. The table (right panel) summarizes statistically significant expression changes by at least 3-fold ($p < 0.05$). (C) The time course of DCPIP-modulation (40 μM) of early growth response protein 1 (EGR1) levels was examined by immunoblot analysis of total cellular protein extracts. Detection of α-actin expression served as a loading control. (C) DCPIP-modulation (20 and 40 μM, 24 h exposure) of cellular heme oxygenase-1 (HO-1) protein levels were examined in total cellular protein extracts by immunoblot analysis. (D) Modulation of cellular Hsp70B' protein levels by DCPIP (1, 10, 20, and 40 μM, 24 h) was examined in total cellular protein extracts followed by ELISA analysis as specified in Section 2 (mean ± SD, $n = 3$). Treatment with celastrol (2 μM, 24 h exposure) was used as a positive control for pharmacological Hsp70B' upregulation.

expression occurred in response to 40 μM DCPIP over untreated controls, with cells exposed to celastrol (2 μM, 24 h) serving as a positive control [41].

3.6. Intraperitoneal administration of DCPIP impairs growth of A375 human melanoma xenografts in SCID mice

The significant apoptogenic and prooxidant stress-inducing activity against A375 melanoma cells combined with a low acute systemic toxicity documented earlier in mice lead us to test DCPIP as a potential inhibitor of tumor growth in a human melanoma SCID-mouse xenograft model (Fig. 7).

Daily intraperitoneal DCPIP treatment (16 mg/kg/d) of human A375 melanoma xenograft bearing SCID mice induced a significant suppression of tumor growth that reached the level of statistical significance ($p < 0.05$ versus PBS treated control) between days 18 and 30 after cell injection, where average tumor weights of DCPIP-treated animals were up to 45% lower than that of carrier-treated controls (Fig. 7A). These data are consistent with impairment of tumor cell proliferative capacity in xenograft-bearing mice treated with DCPIP. However, administration of DCPIP at lower doses (4 mg/kg/d) did not achieve a significant reduction of average tumor weights (Fig. 7A). During DCPIP treatment, no compound-related adverse reactions or statistically significant average weight

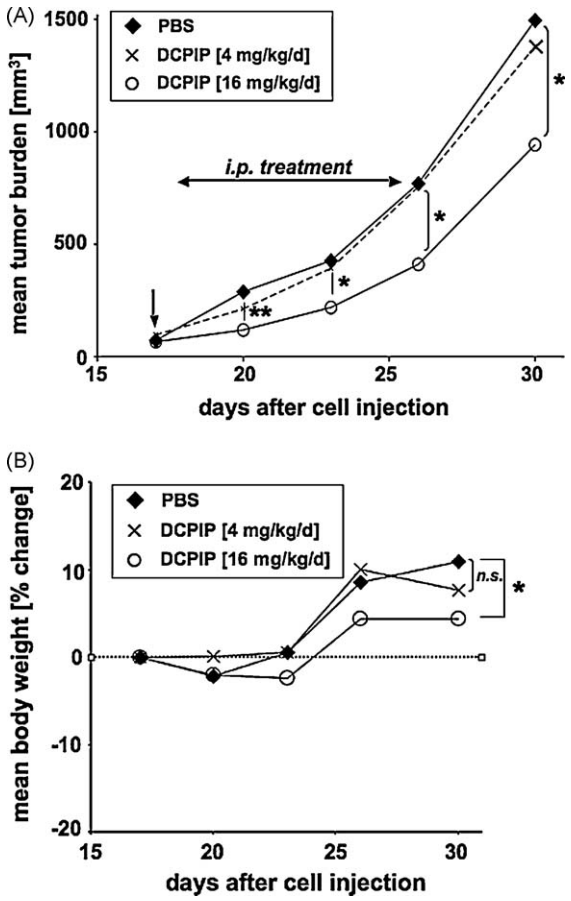

Fig. 7. DCPIP inhibits tumor growth in a human A375 melanoma SCID-mouse xenograft model. Human A375 melanoma cells (10×10^6) were implanted s.c. into the right flank of SCID mice. 17 days after cell injection animals were pair-matched (65 mm^3 average tumor size) and 1 day later (vertical arrow) daily treatment (DCPIP: low dose group: 4 mg/kg/d, 100 μl, q.d., $n = 12$; high dose group: 16 mg/kg/d, 200 μl, b.i.d., $n = 11$) was initiated by intraperitoneal injection as specified in Section 2. Control animals ($n = 12$) received PBS only. (A) Tumor growth curves were obtained by determining average tumor volumes until day 30 after cell injection. Data points are depicted as mean ± SEM and statistical comparison between individual data points was performed using the two-sided Student's *t*-test (*$p < 0.05$; **$p < 0.01$; ***$p < 0.001$). (B) Mean body weight was monitored during the duration of the experiment and expressed as % change from the average weight obtained on the day of pairmatching.

loss were observed suggesting the safety of administration of high doses of DCPIP during the duration of the experiment (Fig. 7B). Moreover, no indication of organ toxicity as revealed by necropsy was obtained (data not shown). However, between days 23 and 30 increase in body average weight was slightly delayed in tumor bearing animals receiving DCPIP-treatment at high (16 mg/kg/d) but not at low (4 mg/kg/d) doses.

Taken together, these findings document for the first time feasibility of antimelanoma intervention by intraperitoneal administration of DCPIP achieved in a mouse xenograft model.

4. Discussion

Metastatic melanoma displays a notorious resistance to conventional chemotherapy, and the current dearth of treatment options creates an urgent need for the development of more efficacious antimelanoma chemotherapeutics [5,42,43]. Based on the well documented preferential sensitivity of melanoma cells to small molecule prooxidant intervention [5,9,14,16,17,20], we tested the feasibility of using the redox-active halogenated benzoquinoneimine-dye DCPIP for melanoma treatment *in vitro* and *in vivo*.

First, we observed that DCPIP induces apoptosis in metastatic human A375, but not in G361 melanoma cells (Figs. 2 and 3). Based on our earlier work that demonstrated differential NQO1 specific enzymatic activity in A375 and G361 cells [14], we then tested the hypothesis that elevated NQO1 expression levels may render G361 melanoma cells resistant to the apoptogenic activity of the prooxidant NQO1-substrate DCPIP. Using the pharmacological NQO1-inhibitor dicoumarol and genetic target modulation by NQO1-siRNA we then obtained strong evidence for the causative role of NQO1 expression in DCPIP-chemoresistance exhibited by G361 human melanoma cells (Figs. 3 and 4). Next, DCPIP-induction of cellular oxidative stress was demonstrated in A375 and G361 melanoma cells assessing cellular peroxide and glutathione levels (Fig. 5). In A375 melanoma cells, intracellular ROS were elevated dose dependently (Fig. 5A) and glutathione levels were lowered significantly within 6 h of exposure (Fig. 5C). Moreover, DCPIP-induced procaspase 3 cleavage could be antagonized by 24 h preincubation of A375 melanoma cells with the thiol antioxidant and glutathione-precursor NAC (Fig. 5B), suggesting the crucial involvement of oxidative stress in DCPIP-induced apoptosis. As seen before, pharmacological or genetic antagonism of NQO1 strongly sensitized G361 cells to DCPIP-induced glutathione depletion (Fig. 5C and D). Consistent with induction of cellular stress by DCPIP treatment, upregulated expression of established oxidative and heat shock stress response genes including HSPA6, HSPA1A, HMOX1, GADD45A, DDIT3, and EGR1 was detected by detailed array analysis (Fig. 6A) [44]. DCPIP-induced upregulation of HSPA6, HMOX1, and EGR1 expression was then confirmed at the protein level using ELISA and Western analysis, respectively (Fig. 6B–D). Remarkably, earlier expression array analysis examining activity of the investigational antimelanoma prooxidant elesclomol against human Hs294T melanoma cells has revealed a similar degree of upregulation of HSPA6 (more than 300-fold) encoding Hsp70B' [17], an Hsp70 subtype not constitutively expressed and induced only under conditions of extreme cellular stress [36]. Moreover, it is tempting to speculate that DCPIP-induced upregulation of the redox sensitive transcription factor EGR1, known to activate expression of tumor suppressor genes including PTEN and TP53, plays a functional role in mediating DCPIP-antimelanoma effects, a hypothesis to be tested by future experiments [37].

Based on these results we then conducted a melanoma xenograft experiment to test DCPIP antimelanoma activity in a relevant animal model of the disease [45]. Daily intraperitoneal administration of DCPIP (16 mg/kg/d) resulted in a significant suppression of tumor growth (Fig. 7A) in a standard A375 human melanoma xenograft SCID mouse model. Importantly, DCPIP administration was well tolerated without induction of significant weight loss over the duration of the experiment (Fig. 7B) or indication of organ toxicity as revealed by necropsy (data not shown). To the best of our knowledge, this is the first report documenting antimelanoma activity of DCPIP *in vivo*.

Numerous prooxidant quinone-derivatives including benzoquinones, naphthoquinones, and tyrosinase-derived acetaminophen-metabolites display anticancer activity that involves induction of oxidative stress [8,30,34,35]. The structure activity relationship of prooxidant quinone-pharmacophores is complex and thought to involve ROS formation via redox cycling and thiol-adduction of protein- and glutathione-cysteine residues [22,46,47]. For example, it is well established that 1,4-benzoquinone, a toxicologically relevant metabolite of benzene, induces oxidative stress in selected target cells including renal proximal tubular epithelial cells through Michael adduction of proteins and glutathione followed by redox cycling of quinol-thioether-adducts [34,48,49]. A considerable body

of prior research has examined redox biochemistry and thiol-adduction associated with DCPIP [27,50,51]. However, the molecular mechanism of DCPIP-induced oxidative stress, evidenced by ROS formation (Fig. 5A), antioxidant protection (Fig. 5B), glutathione depletion (Fig. 5C and D), and upregulated expression of redox sensitive genes (Fig. 6), and its causative role in antimelanoma activity observed *in vivo* remains to be further explored by future experiments. In this context it is interesting to note that the dehalogenated DCPIP-analogue phenolindophenol [4-(4-hydroxyphenyl)-iminocyclohexa-2,5-dien-1-one], when tested by us at equal concentrations as DCPIP, did not display any apoptogenic, caspase 3-activating, or prooxidant activity, and expression of HSPA6, the major stress response gene induced by DCPIP in A375 cells (Fig. 6A), was unchanged (data not shown), suggesting that 2,6-dichloro-substitution is a structural requirement for DCPIP apoptogenicity. Future studies will examine the detailed structure activity relationship between DCPIP-associated cancer cell apoptogenicity and structural parameters including standard reduction potential and electrophilicity providing a basis for rational lead optimization by medicinal chemistry.

In our experiments examining DCPIP apoptogenicity in human A375 and G361 melanoma cells, sensitivity to this treatment was inversely correlated with NQO1 expression levels consistent with the established reductive metabolism of DCPIP and similar quinones by NQO1 known to prevent semiquinone-dependent redox cycling and ROS formation [22,33]. Indeed, considerable chemosensitization of G361 cells displaying high constitutive NQO1 expression levels could be achieved by combining DCPIP treatment with pharmacological or genetic NQO1 inhibition. Similar results were observed in other cancer cell lines previously shown to differ by expression of enzymatically active NQO1: e.g., MIA-PaCa-2 pancreas carcinoma cells with high specific NQO1 activity displayed pronounced DCPIP chemoresistance, whereas MDA-MB231 breast carcinoma cells, known to display the NQO1*2 genotype resulting in negligible NQO1 specific enzymatic activity [14,33], were highly sensitive to DCPIP apoptogenicity (data not shown). Taken together, these data suggest that expression of active NQO1 protects against DCPIP-quinoneimine associated oxidative stress and cytotoxicity and is therefore an important determinant and predictor of DCPIP chemosensitivity of cancer cells.

Only limited information is currently available on NQO1 expression and activity levels in human metastatic melanoma. In our earlier experiments performed in cultured human metastatic melanoma cell lines (G361, LOX, A375) [14], high NQO1 activity was observed in G361 and LOX cells, whereas low activity was detected in A375 cells, a cell line widely employed in many standard xenograft models for the identification of potential antimelanoma agents [45]. In another study, a spectrum of NQO1 activities ranging from high to very low was reported (in that order) for SKMEL5, WM266.4, SKMEL 28, and SKMEL 2 human melanoma cells [52]. In conjunctival melanomas and primary acquired melanosis immunohistochemical detection of NQO1 was performed recently, but no enzymatic activity was assessed [53].

Importantly, constitutive NQO1 overexpression leading to high specific enzymatic activity is associated with various human malignancies including non-small cell lung cancer, pancreas carcinoma, and colon adenocarcinoma [54,55], and it has long been known that tumors that display high NQO1 enzymatic activity can be targeted by NQO1-dependent bioreductively activated anticancer agents including alkylating agents such as mitomycin C and aziridinylbenzoquinones [33]. In contrast, other tumors, including glioblastoma [56], leukemia [57], lymphoma [58], and breast carcinoma [59], may display impaired expression of functional NQO1 resulting in very low or absent NQO1 activity [33]. Moreover, it has recently been demonstrated that a homozygous common missense genotype [NQO1(*)2, NM_000903.2:c.558C>T] encoding the functionally impaired NQO1 P187S protein, rapidly degraded via the ubiquitin proteasomal pathway, strongly predicts poor survival among women with breast cancer [59]. Remarkably, the NQO1*2 missense variant (NP_000894:p.187P4S) is homozygous in 4–20% of the human population. Moreover, response to the anthracycline tumor antibiotic epirubicin is impaired in NQO1(*)2-homozygous breast carcinoma cells *in vitro*, suggesting that this NQO1-genotype is a prognostic and predictive marker for breast cancer chemotherapy.

Our results that demonstrate feasibility of DCPIP-based chemotherapy of A375 melanoma suggest that DCPIP or improved derivatives may target human melanoma or other tumors (including breast carcinoma and lymphoma) that display low NQO1 enzymatic activity, a hypothesis to be tested by future experiments. Moreover, feasibility of sensitization of G361 melanoma cells to DCPIP cytotoxicity by pharmacological or genetic NQO1 antagonism as demonstrated in this study suggests that combination therapy employing a member of the rapidly expanding group of non-cytotoxic NQO1 inhibitors together with a DCPIP-like molecule may provide therapeutic efficacy against tumors that display high NQO1 enzymatic activity [60].

Based on the significant antimelanoma activity of DCPIP observed here at well-tolerated intraperitoneal doses, future preclinical studies will further examine the mostly unexplored anticancer and safety profile of this experimental redox chemotherapeutic.

Acknowledgements

Supported in part by grants from the National Institutes of Health [R01CA122484, ES007091, ES06694, Arizona Cancer Center Support Grant CA023074], and from the Arizona Biomedical Research Commission (ABRC 0721). Animal experimentation was performed at the AZCC experimental mouse shared service (EMSS).

References

[1] Laurent A, Nicco C, Chereau C, Goulvestre C, Alexandre J, Alves A, et al. Controlling tumor growth by modulating endogenous production of reactive oxygen species. Cancer Res 2005;65:948–56.
[2] Hileman EO, Liu J, Albitar M, Keating MJ, Huang P. Intrinsic oxidative stress in cancer cells: a biochemical basis for therapeutic selectivity. Cancer Chemother Pharmacol 2004;53:209–19.
[3] Cabello CM, Bair III WB, Wondrak GT. Experimental therapeutics: targeting the redox Achilles heel of cancer. Curr Opin Investig Drugs 2007;8:1022–37.
[4] Fruehauf JP, Meyskens Jr FL. Reactive oxygen species: a breath of life or death? Clin Cancer Res 2007;13:789–94.
[5] Fruehauf JP, Trapp V. Reactive oxygen species: an Achilles' heel of melanoma? Expert Rev Anticancer Ther 2008;8:1751–7.
[6] Efferth T. Mechanistic perspectives for 1,2,4-trioxanes in anti-cancer therapy. Drug Resist Update 2005;8:85–97.
[7] Efferth T. Molecular pharmacology and pharmacogenomics of artemisinin and its derivatives in cancer cells. Curr Drug Targets 2006;7:407–21.
[8] Verrax J, Stockis J, Tison A, Taper HS, Calderon PB. Oxidative stress by ascorbate/menadione association kills K562 human chronic myelogenous leukaemia cells and inhibits its tumour growth in nude mice. Biochem Pharmacol 2006;72: 671–80.
[9] Loewe R, Valero T, Kremling S, Pratscher B, Kunstfeld R, Pehamberger H, et al. Dimethylfumarate impairs melanoma growth and metastasis. Cancer Res 2006;66:11888–96.
[10] Wang CC, Chiang YM, Sung SC, Hsu YL, Chang JK, Kuo PL. Plumbagin induces cell cycle arrest and apoptosis through reactive oxygen species/c-Jun N-terminal kinase pathways in human melanoma A375.S2 cells. Cancer Lett 2008;259:82–98.
[11] Cabello CM, Bair III WB, Lamore SD, Bause AS, Azimian S, Wondrak GT. The cinnamon-derived Michael acceptor cinnamic aldehyde impairs melanoma cell proliferation, invasiveness, and tumor growth. Free Radic Biol Med 2009;46:220–31.
[12] Fry FH, Holme AL, Giles NM, Giles GI, Collins C, Holt K, et al. Multifunctional redox catalysts as selective enhancers of oxidative stress. Org Biomol Chem 2005;3:2579–87.

[13] Magda D, Miller RA. Motexafin gadolinium: a novel redox active drug for cancer therapy. Semin Cancer Biol 2006;16:466–76.
[14] Wondrak GT. NQO1-activated phenothiazinium redox cyclers for the targeted bioreductive induction of cancer cell apoptosis. Free Radic Biol Med 2007;43:178–90.
[15] Berger TG, Dieckmann D, Efferth T, Schultz ES, Funk JO, Baur A, et al. Artesunate in the treatment of metastatic uveal melanoma—first experiences. Oncol Rep 2005;14:1599–603.
[16] Cen D, Brayton D, Shahandeh B, Meyskens Jr FL, Farmer PJ. Disulfiram facilitates intracellular Cu uptake and induces apoptosis in human melanoma cells. J Med Chem 2004;47:6914–20.
[17] Kirshner JR, He S, Balasubramanyam V, Kepros J, Yang CY, Zhang M, et al. Elesclomol induces cancer cell apoptosis through oxidative stress. Mol Cancer Ther 2008;7:2319–27.
[18] Tuma RS. Reactive oxygen species may have antitumor activity in metastatic melanoma. J Natl Cancer Inst 2008;100:11–2.
[19] Brar SS, Kennedy TP, Sturrock AB, Huecksteadt TP, Quinn MT, Whorton AR, et al. An NAD(P)H oxidase regulates growth and transcription in melanoma cells. Am J Physiol Cell Physiol 2002;282:C1212–24.
[20] Wittgen HG, van Kempen LC. Reactive oxygen species in melanoma and its therapeutic implications. Melanoma Res 2007;17:400–9.
[21] Fried L, Arbiser JL. The reactive oxygen-driven tumor: relevance to melanoma. Pigment Cell Melanoma Res 2008;21:117–22.
[22] Criddle DN, Gillies S, Baumgartner-Wilson HK, Jaffar M, Chinje EC, Passmore S, et al. Menadione-induced reactive oxygen species generation via redox cycling promotes apoptosis of murine pancreatic acinar cells. J Biol Chem 2006;281:40485–92.
[23] Ernster L. DT-diaphorase. Methods Enzymol 1967;10:309–17.
[24] Wilson GS. Determination of oxidation–reduction potentials. Methods Enzymol 1978;54:396–410.
[25] VanderJagt DJ, Garry PJ, Hunt WC. Ascorbate in plasma as measured by liquid chromatography and by dichlorophenolindophenol colorimetry. Clin Chem 1986;32:1004–6.
[26] Yamashita T, Butler WL. Photoreduction and photophosphorylation with tris-washed chloroplasts. Plant Physiol 1968;43:1978–86.
[27] Mayer D, Naumann R, Edler L, Bannasch P. Investigation by amperometric methods of intracellular reduction of 2,6-dichlorophenolindophenol in normal and transformed hepatocytes in the presence of different inhibitors of cellular metabolism. Biochim Biophys Acta 1990;1015:258–63.
[28] Kumar S, Acharya SK. 2,6-Dichloro-phenol indophenol prevents switch-over of electrons between the cyanide-sensitive and -insensitive pathway of the mitochondrial electron transport chain in the presence of inhibitors. Anal Biochem 1999;268:89–93.
[29] Wolchok JD, Williams L, Pinto JT, Fleisher M, Krown SE, Hwu WJ, et al. Phase I trial of high dose paracetamol and carmustine in patients with metastatic melanoma. Melanoma Res 2003;13:189–96.
[30] Vad NM, Yount G, Moore D, Weidanz J, Moridani MY. Biochemical mechanism of acetaminophen (APAP) induced toxicity in melanoma cell lines. J Pharm Sci 2009;98:1409–25.
[31] MSDS: 2,6-Dichloroindophenol sodium salt (CAS#620-45-1). *Sigma-Aldrich* Version 1.5, 01/31/2006.
[32] Wondrak GT, Jacobson MK, Jacobson EL. Antimelanoma activity of apoptogenic carbonyl scavengers. J Pharmacol Exp Ther 2006;316:805–14.
[33] Ross D, Siegel D. NAD(P)H:quinone oxidoreductase 1 (NQO1, DT-diaphorase), functions and pharmacogenetics. Methods Enzymol 2004;382:115–44.
[34] Baigi MG, Brault L, Neguesque A, Beley M, Hilali RE, Gauzere F, et al. Apoptosis/necrosis switch in two different cancer cell lines: influence of benzoquinone- and hydrogen peroxide-induced oxidative stress intensity, and glutathione. Toxicol In Vitro 2008;22:1547–54.
[35] Fukuyo Y, Inoue M, Nakajima T, Higashikubo R, Horikoshi NT, Hunt C, et al. Oxidative stress plays a critical role in inactivating mutant BRAF by geldanamycin derivatives. Cancer Res 2008;68:6324–30.
[36] Noonan E, Giardina C, Hightower L. Hsp70B' and Hsp72 form a complex in stressed human colon cells and each contributes to cytoprotection. Exp Cell Res 2008;314:2468–76.
[37] Baron V, Adamson ED, Calogero A, Ragona G, Mercola D. The transcription factor Egr1 is a direct regulator of multiple tumor suppressors including TGFbeta1, PTEN, p53, and fibronectin. Cancer Gene Ther 2006;13:115–24.
[38] Shen Y, Wang J, Yang T, Li Y, Jiang W, Guan Z, et al. Platinums sensitize human epithelial tumor cells to lymphotoxin alpha by inhibiting NFkappaB-dependent transcription. Cancer Biol Ther 2008;7:1407–14.
[39] Sarkar D, Su ZZ, Lebedeva IV, Sauane M, Gopalkrishnan RV, Valerie K, et al. mda-7 (IL-24) Mediates selective apoptosis in human melanoma cells by inducing the coordinated overexpression of the GADD family of genes by means of p38 MAPK. Proc Natl Acad Sci USA 2002;99:10054–9.
[40] Scott DW, Loo G. Curcumin-induced GADD153 gene up-regulation in human colon cancer cells. Carcinogenesis 2004;25:2155–64.
[41] Chow AM, Brown IR. Induction of heat shock proteins in differentiated human and rodent neurons by celastrol. Cell Stress Chaperones 2007;12:237–44.
[42] Wondrak GT, Jacobson MK, Jacobson EL. An emerging molecular target in melanoma: cellular carbonyl stress and the inhibition of mitochondrial survival pathways by carbonyl scavenger agents. Curr Cancer Ther Rev 2005;1:271–6.
[43] Hocker TL, Singh MK, Tsao H. Melanoma genetics and therapeutic approaches in the 21st century: moving from the benchside to the bedside. J Invest Dermatol 2008;128:2575–95.
[44] Han ES, Muller FL, Perez V, Qi W, Liang H, Xi L, et al. The in vivo gene expression signature of oxidative stress. Physiol Genomics 2008.
[45] Paine-Murrieta GD, Taylor CW, Curtis RA, Lopez MH, Dorr RT, Johnson CS, et al. Human tumor models in the severe combined immune deficient (scid) mouse. Cancer Chemother Pharmacol 1997;40:209–14.
[46] Abdelmohsen K, Gerber PA, von Montfort C, Sies H, Klotz LO. Epidermal growth factor receptor is a common mediator of quinone-induced signaling leading to phosphorylation of connexin-43: role of glutathione and tyrosine phosphatases. J Biol Chem 2003;278:38360–7.
[47] Schmieder PK, Tapper MA, Kolanczyk RC, Hammermeister DE, Sheedy BR, Denny JS. Discriminating redox cycling and arylation pathways of reactive chemical toxicity in trout hepatocytes. Toxicol Sci 2003;72:66–76.
[48] Lau SS, Hill BA, Highet RJ, Monks TJ. Sequential oxidation and glutathione addition to 1,4-benzoquinone: correlation of toxicity with increased glutathione substitution. Mol Pharmacol 1988;34:829–36.
[49] Bratton SB, Lau SS, Monks TJ. The putative benzene metabolite 2,3, 5-tris(-glutathion-S-yl)hydroquinone depletes glutathione, stimulates sphingomyelin turnover, and induces apoptosis in HL-60 cells. Chem Res Toxicol 2000;13:550–6.
[50] Hadler HI, Alt SK, Falcone AB. Conjugation of 2,6-dichloroindophenol with mitochondrial thiol groups. J Biol Chem 1966;241:2886–90.
[51] Dupuy C, Kaniewski J, Ohayon R, Deme D, Virion A, Pommier J. Nonenzymatic NADPH-dependent reduction of 2,6-dichlorophenol-indophenol. Anal Biochem 1990;191:16–20.
[52] Sharp SY, Boxall K, Rowlands M, Prodromou C, Roe SM, Maloney A, et al. In vitro biological characterization of a novel, synthetic diaryl pyrazole resorcinol class of heat shock protein 90 inhibitors. Cancer Res 2007;67:2206–16.
[53] Wilson MW, Schelonka LP, Siegel D, Meininger A, Ross D. Immunohistochemical localization of NAD(P)H:quinone oxidoreductase in conjunctival melanomas and primary acquired melanosis. Curr Eye Res 2001;22:348–52.
[54] Danson S, Ward TH, Butler J, Ranson M. DT-diaphorase: a target for new anticancer drugs. Cancer Treat Rev 2004;30:437–49.
[55] Lewis AM, Ough M, Hinkhouse MM, Tsao MS, Oberley LW, Cullen JJ. Targeting NAD(P)H:quinone oxidoreductase (NQO1) in pancreatic cancer. Mol Carcinog 2005;43:215–24.
[56] Seng S, Avraham HK, Birrane G, Jiang S, Li H, Katz G, et al. NRP/B mutations impair Nrf2-dependent NQO1 induction in human primary brain tumors. Oncogene 2009;28:378–89.
[57] Wiemels JL, Pagnamenta A, Taylor GM, Eden OB, Alexander FE, Greaves MF. A lack of a functional NAD(P)H:quinone oxidoreductase allele is selectively associated with pediatric leukemias that have MLL fusions. United Kingdom Childhood Cancer Study Investigators. Cancer Res 1999;59:4095–9.
[58] Bruge F, Virgili S, Cacciamani T, Principi F, Tiano L, Littarru GP. NAD(P)H:quinone oxidoreductase (NQO1) loss of function in Burkitt's lymphoma cell lines. Biofactors 2008;32:71–81.
[59] Fagerholm R, Hofstetter B, Tommiska J, Aaltonen K, Vrtel R, Syrjakoski K, et al. NAD(P)H:quinone oxidoreductase 1 NQO1*2 genotype (P187S) is a strong prognostic and predictive factor in breast cancer. Nat Genet 2008;40:844–53.
[60] Nolan KA, Timson DJ, Stratford IJ, Bryce RA. In silico identification and biochemical characterization of novel inhibitors of NQO1. Bioorg Med Chem Lett 2006;16:6246–54.